Linköping Studies in Science and Technology.
Licentiate Thesis No. 1571

Stress and fatigue constrained topology optimization

Erik Holmberg

Linköping University
INSTITUTE OF TECHNOLOGY

LIU–TEK–LIC–2013:5

Department of Management and Engineering, Division of Mechanics
Linköping University, SE–581 83, Linköping, Sweden

Linköping, February 2013

Cover:
L-shaped beam, optimized for minimum mass subjected to stress constraints.

Printed by:
LiU-Tryck, Linköping, Sweden, 2013
ISBN 978-91-7519-703-6
ISSN 0280-7971

Distributed by:
Linköping University
Department of Management and Engineering
SE–581 83, Linköping, Sweden

This document was prepared with LaTeX, January 3, 2013

Preface

The work presented in this licentiate thesis has been carried out at Saab AB and at the Division of Mechanics, Linköping University. The research has been funded by Vinnova, within NFFP5 (Nationella Flygtekniska ForskningsProgrammet).

I would like to thank my supervisors, Anders Klarbring and Bo Torstenfelt, for all their guiding and help during the work that has led to this thesis. I would also like to thank colleagues at Saab AB and Linköping University for support, encouragement and interesting work-related, as well as off-topic, discussions. Finally, I would like to thank to my friends and family, especially my lovely fiancée Elina, for daily support and for making every day a joy.

Erik Holmberg

Linköping, December 2012

Abstract

This thesis concerns structural optimization in conceptual design stages, for which constraints that are adapted to industrial requirements have been developed for topology optimization problems. The objective of the project has been to identify and solve problems that today prevent structural optimization from being used in a broader sense in the avionic industry; the main focus has been on stress and fatigue constraints in topology optimization.

The thesis consists of two parts. The first part gives an introduction to topology optimization and describes the developed methods for stress and fatigue constraints. In the second part, two papers are included, where the stress and fatigue constraints are evaluated, respectively.

In the first paper, a clustered approach is presented, where stress constraints are applied to stress clusters, rather than points on the structure. This allows for a trade-off between computational time and accuracy, as the number of clusters and thus constraints can be varied. Different approaches for how to sort stress evaluation points into clusters and how to update the clusters, such that the results are sufficiently accurate for conceptual designs, are developed and evaluated. The two-dimensional examples confirm the theoretical discussions and the designs that are obtained have managed to avoid large stress concentrations, even for problems with an initial stress singularity. Compared to the traditional stiffness based designs, the stress constrained designs are considered to be closer to a final design, which will decrease the total product development time.

The second paper uses the methodology developed in the first paper and applies it to high-cycle fatigue constraints. Using loads described by a variable load spectrum and material data from fatigue tests, the tensile principal stresses are constrained by a limit that is determined such that fatigue failure will not occur. In the examples, where the mass is minimized subjected to fatigue and static stress constraints, simple topologies are obtained and the structural parts are sized with respect to the critical fatigue stress and the yield limit. Stress concentrations are again avoided, for example by the creation of a radius around an internal corner. A comparison between static stress constraints based on the von Mises criterion and the highest tensile principal stresses is given and the examples clearly show the characteristics of the two formulations.

List of Papers

The following two papers have been included in this thesis:

I. E. Holmberg, B. Torstenfelt, A. Klarbring (2012). *Stress constrained topology optimization*. Accepted for publication.

II. E. Holmberg, B. Torstenfelt, A. Klarbring. *Fatigue constrained topology optimization*. To be submitted.

Own contribution

In both listed papers I have been the main contributor for writing, modelling and running the optimizations. The main part of the implementation is made together with Bo Torstenfelt and the mathematical formulations are created together with Anders Klarbring.

Contents

Part I

Theory and background

1 Introduction

1.1 Structural optimization in the product development process

Light weight designs are desirable in many industrial applications; it is of particular interest in the avionic industry, but also in the development of cars, trucks and sports equipment among other applications. By introducing structural optimization in the product development process, a lighter design can be achieved without necessarily increasing the amount of required work. Actually, if the structural optimization is well incorporated with the methods used for product development, the process can be made much faster than conventional product development, as manual iterations between designers and stress engineers are removed or at least reduced. A simplified flowchart of the product development process is shown in Figure 1 and it can be compared to the flowchart for manual design in Figure 2; at least one step is added, but the need for time consuming manual adjustments is reduced.

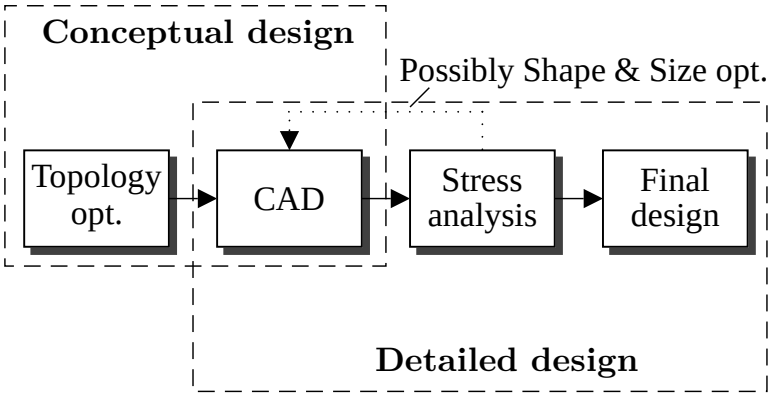

Figure 1: Simplified product development process, using topology optimization with stress and fatigue constraints.

The work presented in this thesis strives for generating lighter designs in a con-

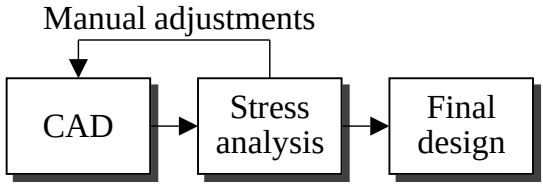

Figure 2: Simplified manual product development process, without any optimization.

ceptual design phase. This is achieved by the use of topology optimization with constraints that correspond to the requirements that the industry apply to a structure. We minimize the mass while creating load carrying structures and the focus is on the avionic industry, even though the developed methods apply to a large variety of industrial applications. In the avionic industry (both military and civil), lighter designs have many positive effects on performance and concerning environmental aspects. The immediate results of using structural optimization to generate lighter designs are:

- Better performance,
- Increased pay-load,
- Longer range,
- Reduced emission of CO_2.

Further positive effects are reduction of working time and thus development costs.

1.2 Topology optimization

Topology optimization is the most general structural optimization technique and it is mainly considered in a conceptual design stage. The Greek word *topos*, meaning landscape or place, is the origin of the word *topology* optimization, [45]. Compared to size and shape optimization, topology optimization allows more freedom as no initial structure is required. Only the design space, the loads and the boundary conditions are required in order to find an optimized structure which satisfies the given constraints.

In topology optimization a fixed finite element mesh is used and one design variable is connected to each element. The design variable determines if the corresponding element will represent structural material or a hole. The connectivity of the structure, while connecting the applied loads to the given boundary conditions, is thus changed such that the objective function is minimized subjected to the specified constraints.

1.3 Historical background and milestones

The first steps towards what today is called topology optimization were made in the mid 1960s, when a number of papers on optimization of truss structures were published, e.g. by Dorn et al. [20]. Optimization in the form of pointwise material or voids in two dimensional applications was introduced by Kohn and Strang in 1986 [51], [31].

The concept of topology optimization that is used today, i.e. penalization of intermediate design variable values, in order to achieve a design with only solid material and voids, was introduced by Bendsøe in 1989 [3]. The approach in [3] was made possible due to the work by Bendsøe and Kikuchi from 1988 [5].

The introduction of filters is another major step in the history of topology optimization. Filters made the results better, in the sense that final structures became easier to interpret and bad FE-modelling was avoided, details will be discussed in Section 2.2. There are mainly two types of filters, the first was introduced by Sigmund in the mid 1990s [44] and the second by Bruns and Tortorelli 2001 [11]. The filter developed by Sigmund uses a heuristic approach, where the sensitivity with respect to a design variable is changed based on the sensitivity with respect to neighbouring design variables. The filter by Bruns and Tortorelli changes the design variables $\boldsymbol{x}$ into filtered variables $\boldsymbol{\rho}(\boldsymbol{x})$ by weighting each design variable value with the values of neighbouring design variables.

2 Discretization of the continuum problem

In structural topology optimization, the Finite Element Method, see e.g. [26] or [16], is used to discretize the continuum problem and to solve the static equilibrium problem. The finite element mesh is also used to define the design variables. The continuum problem is defined on the design domain Ω, which in topology optimization often has a box shape, as in Figure 3, within which the structure should be contained. We restrict this work to isotropic materials and four-node quadrilateral elements are used in the examples, even though the method is not restricted to this element type, as discussed in Section 6.1.

2.1 Design variables

One design variable, x_e, is used for each finite element that discretizes the design domain Ω. The design variables are bounded by box constraints $0 < \epsilon \leq x_e \leq 1$, where ϵ is a small value which prevents that the local stiffness goes to zero when the design variable approaches its lower bound. A vanishing stiffness would cause numerical instabilities, which will be discussed more in Section 2.3.

The design variable is a scale factor of element properties, where ϵ implies that the element represents a hole and one implies that the element represents solid material. Thus, the design variables determine the connectivity of the structure within the given design domain. Usually, a final design which contains only solid material and holes is required, as this represents a structure with homogenous material properties. The design variables are continuous and intermediate design variable values are therefore penalized in order to make these unproportionately expensive in terms of structural responses. The intermediate values will therefore be unfavoured by the optimization and thus avoided in the final design.

How to interpret the design variables physically has been an object of many discussions. Among the most popular interpretations are element thickness in 2D-problems [40], material density [7], [8], [44], [9] or as composite material [6] in the form of porosity or layered materials. Due to the lack of a clear physical interpretation, the method was called artificial or fictious material optimization, until Bendsøe and Sigmund [6] showed that composite materials can be used to physically interpret the intermediate values. However, such a material, with pointwise

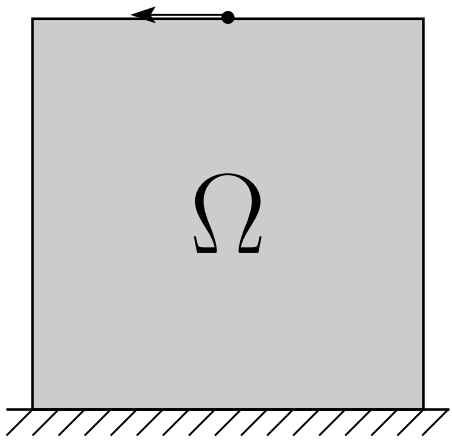

Figure 3: A typical design domain Ω and boundary conditions for a topology optimization problem.

different properties, does not correspond to the usual materials used for load carrying structures. In this work we do not give a physical interpretation of the design variables, but see them as mathematical scale factors of element properties. Actually, no physical interpretation of intermediate design variable values is required, as we expect to obtain a final design representing only solid material and voids.

Using a lower bound, $\epsilon > 0$, on the design variables is an accepted method in the literature and it is used by most authors. However, methods for using a zero-valued lower bound are discussed by some authors: Kočvara [30] optimized trusses and allowed the volume of the bars to be zero, i.e. allowed the stiffness matrix to become singular and solved the singularity problem by using generalized inverses. A drawback was that the computation of a generalized inverse was much more costly than the computation of the inverse of a non-singular matrix. Washizawa et al. [59] used the conjugate gradient method and the conjugate residual method to iteratively achieve values even though the stiffness matrix was singular. Zero bounds have also been discussed by Bendsøe et al. [4] where the simultaneous approach was used, i.e. the global state equation was considered as an equilibrium constraint and both the displacements and the design variables were solved for in the optimization. Therefore, the global stiffness matrix did not have to be assembled. Bruns [10] suggested a heuristic method and generated smooth solutions to the state problem in a node surrounded by void elements by numerically suppressing its degrees of freedom. Using this technique, the element stiffness matrix did not have to be assembled for zero-valued design variables. Instead, the corresponding position of the global stiffness matrix was put to one on the diagonal and the corresponding position of the load vector was set to zero, in order to ensure that the displacement would become zero. Thus, the problem with infinite number of solutions that occurs when the stiffness matrix becomes singular was avoided. The method was

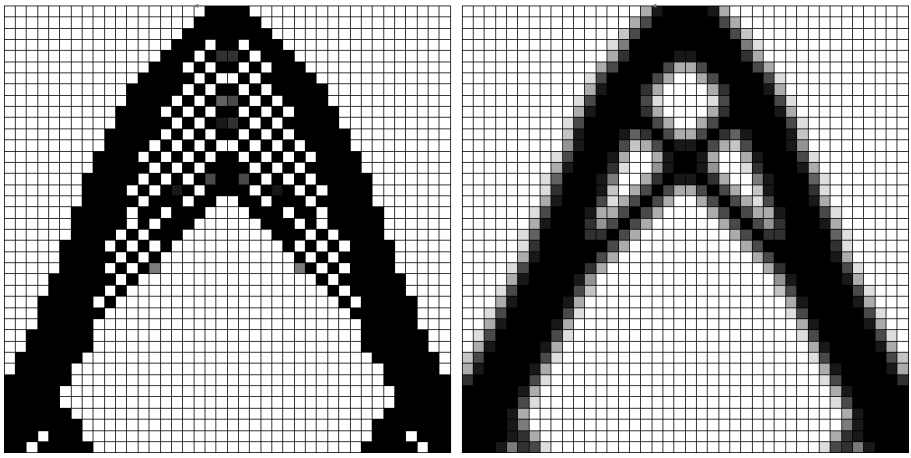

Figure 4: Left: No filter and thus checkerboards. Right: A design variable filter with radius 1.5 times element size; no checkerboards appear but a transition layer (grey) between solid and void remains in the final design.

shown for truss designs and for a 2D compliance optimization problem.

2.2 Filtering techniques

Filters are introduced in topology optimization in order to remove checkerboard patterns and mesh dependency, [48]. Checkerboard pattern refers to a solution where the material is distributed in a pattern that varies between solid and void in consecutive elements. Thus, if solid material is displayed in black and voids are displayed in white, the material distribution looks like a checkerboard, as seen in the left example in Figure 4. When four-node quadrilateral elements are used (which is very common in topology optimization and also used in this work), the stiffness for a checkerboard becomes very high and is therefore favoured by the optimization. Díaz and Sigmund [19] proved that the high stiffness is artificial and due to bad modelling, thus not a representation of an optimal material distribution. Mesh dependency implies that different solutions are obtained for different discretizations; typically, smaller elements lead to an increasing number of thinner structural parts.

Mainly two types of filters are used in topology optimization: the sensitivity filter developed by Sigmund [44] and the design variable filter (often called density filter) developed by Bruns and Tortorelli [11]. The sensitivity filter modifies the derivatives in a heuristic way, that is, there is no mathematical proof of the theory. Thus, it cannot be established what the optimization problem to be solved looks like, as the derivatives are not consistent with the problem formulation. However, several

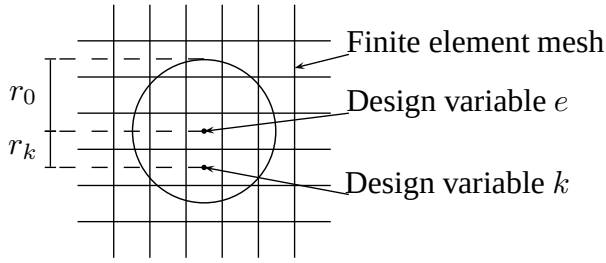

Figure 5: Visualization of a filter for design variable x_e.

tests in different applications have shown that the filter gives good solutions. The sensitivity filter in [44] reads

$$\frac{\widehat{\partial f}}{\partial x_e} = \frac{\sum_{k=1}^{n_e} w_k x_k \frac{\partial f}{\partial x_k}}{x_e \sum_{k=1}^{n_e} w_k}, \tag{1}$$

where f is the objective or a constraint function, n_e is the number of design variables and w_k is the mesh-independent convolution operator, or simply, the weight factor. The weight factor is in this work defined by a cone, i.e. the weight decreases linearly with the distance and the weight factor reads

$$w_k = \frac{r_0 - r_k}{r_0}, \tag{2}$$

where r_0 is the filter radius and r_k is the distance from the centroid of element e to the centroid of element k, see Figure 5. The weight factor is zero if the distance is greater than the filter radius r_0.

The density filter is more straight forward mathematically. Filtered variables, $\rho_e(\boldsymbol{x})$, are created by taking a weighted average of neighbouring design variables x_k. The sensitivities are calculated based on the filtered variables and when the design variables have been updated, new filtered variable values are calculated again. The density filter formulation in [11] looks like

$$\rho_e(\boldsymbol{x}) = \frac{\sum_{k \in \Omega_e} w_k x_k}{\sum_{k \in \Omega_e} w_k}, \tag{3}$$

where the domain Ω_e includes all the design variables within the filter radius r_0 and w_k is given by (2). Common for both filter techniques is the drawback that a grey area is created between black and white, i.e. the final solution will always contain a transition region of intermediate design variable values on the boundaries of the structure, see the right example in Figure 4. This problem is not addressed in this work. Several ways to remove this transition region has been suggested in the literature and a comprehensive review and comparison is presented by Sigmund [46]. The design variable filter (3) is used in this work.

2.3 Penalization techniques

In order to create black-and-white structures, i.e. having design variable values 1 (black) and ϵ (white) and no intermediate (grey) design variable values, intermediate densities are penalized, i.e. made more expensive. The penalization can be added to influence for example the stiffness, the stresses or the volume and the two first are used in this work. Due to the penalization, the element properties for intermediate design variable values are non-physical. However, as discussed in Section 2.1, the purpose of using penalization is to find a black-and-white solution, for which the penalization functions have no influence. Examples of penalization functions are shown in Figure 6 and described below.

2.3.1 Stiffness penalization

The penalization of stiffness was initially introduced by Bendsøe [3] and it was later named SIMP by Rozvany [43]. SIMP, meaning Solid Isotropic Material with Penalization, is the most well known penalization method and it is still used by most authors. An extensive historical discussion of the SIMP method is given by Rozvany in [40] and [41], to which the interested reader is referred.

The SIMP penalization function, $\eta_K(\rho_e(\boldsymbol{x}))$, is inserted when the global stiffness matrix $\boldsymbol{K}(\boldsymbol{\rho}(\boldsymbol{x}))$ is assembled from the solid material element stiffness matrices $\boldsymbol{K}_e$ as

$$\boldsymbol{K}(\boldsymbol{\rho}(\boldsymbol{x})) = \sum_{e=1}^{n_e} \eta_K(\rho_e(\boldsymbol{x}))\,\boldsymbol{K}_e, \tag{4}$$

and it is given by

$$\eta_K(\rho_e(\boldsymbol{x})) = (\rho_e(\boldsymbol{x}))^q, \tag{5}$$

where $q > 1$ is a penalization factor that is usually set to $q = 3$, which by several authors has been proven to work well. In (4) it is understood why the lower bound ϵ on the design variables was introduced in Section 2.1; if $\rho_e(\boldsymbol{x}) = 0$ the stiffness matrix may become singular. The lower bound ϵ has to be such that inserted into (5) the penalization function $\eta_K(\rho_e(\boldsymbol{x})) = \epsilon^q$ is small enough so that the structural analysis is not affected and large enough to avoid singularity of the stiffness matrix. Bendsøe and Sigmund [2] recommend a typical value about $\epsilon = 10^{-3}$; we have used $\epsilon = 0.5 \times 10^{-2}$ throughout all calculations.

Other similar penalization methods exist. Stolpe and Svanberg [50] developed another stiffness penalization called RAMP, Rational Approximation of Material Properties, where the penalization instead reads

$$\eta_K^{\text{RAMP}}(\rho_e(\boldsymbol{x})) = \frac{\rho_e(\boldsymbol{x})}{1 + q(1 - \rho_e(\boldsymbol{x}))},$$

which has a nonzero gradient when $\rho_e(\boldsymbol{x}) = 0$. In combination with the introduction of a minimum element stiffness, RAMP allows for a zero-valued lower bound on the design variables. Another penalization method that also shares the non disappearing gradients is the SINH method developed by Bruns [9]. In the SINH method, the actual design variable value is used to calculate the stiffness and instead the volume is penalized by a function $\eta_V(\rho_e(\boldsymbol{x}))$, defined as

$$\eta_V(\rho_e(\boldsymbol{x})) = 1 - \frac{\sinh(q(1-\rho_e(\boldsymbol{x})))}{\sinh(q)}.$$

The intermediate design variable values are thus less effective from a volumetric point of view. A combination of SIMP and SINH, called hybrid SINH is also discussed in [9], where the structural analysis is based on the SIMP penalization and the volume calculation is based on the SINH penalization.

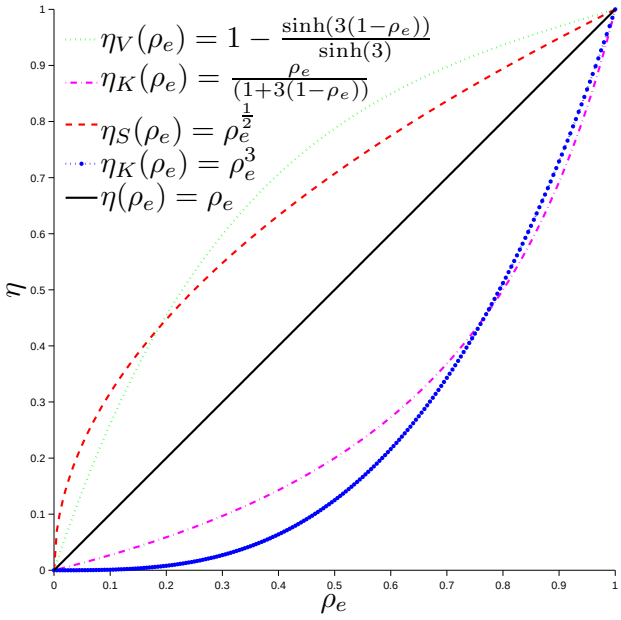

Figure 6: Different penalization functions.

2.3.2 Stress penalization

The SIMP method for penalization of the structural stiffness has become an accepted method for compliance based problems. In addition to the stiffness penal-

ization we also penalize the stress for intermediate design variable values. Duysinx and Bendsøe [21] scaled the stresses such that the local stress was consistent with the local stiffness, which generated singularity problems (stress singularity is discussed in Section 4.1) which were avoided by the use of the ϵ-relaxation approach, developed by Cheng and Guo [14]. However, as the goal with the penalization is to achieve a final design without intermediate design variables, there is no need for the stresses to be consistent with the stiffness, which anyhow, does not represent a physical stiffness due to the penalization. This was used by Bruggi [8] in the so-called qp-approach where a stress penalization was used with another exponent than in the stiffness penalization. This gave the desired property that the stress $\sigma(\boldsymbol{x}) \to 0$ when $x \to 0$ and thus, no singularity problem. A similar penalization technique but with a fixed exponent was used by Le et al. [32] and the same stress penalization technique is used in Paper 1 and Paper 2. The stress penalization for design variable x_e, $\eta_S(\rho_e(\boldsymbol{x}))$, reads

$$\eta_S(\rho_e(\boldsymbol{x})) = (\rho_e(\boldsymbol{x}))^{\frac{1}{2}}. \tag{6}$$

The solid material stress tensor for stress evaluation point a, where a belongs to the element connected to the e:th design variable, is expressed in Voigt notation,

$$\hat{\boldsymbol{\sigma}}_a(\boldsymbol{x}) = \begin{pmatrix} \hat{\sigma}_{ax} & \hat{\sigma}_{ay} & \hat{\sigma}_{az} & \hat{\tau}_{axy} & \hat{\tau}_{ayz} & \hat{\tau}_{azx} \end{pmatrix}^T$$

and it is calculated by the finite element analysis (FE-analysis), as

$$\hat{\boldsymbol{\sigma}}_a(\boldsymbol{x}) = \boldsymbol{E}\boldsymbol{B}_a\boldsymbol{u}(\boldsymbol{x}),$$

where $\boldsymbol{E}$ is the constitutive matrix, $\boldsymbol{B}_a$ is the strain-displacement matrix corresponding to stress evaluation point a and $\boldsymbol{u}(\boldsymbol{x})$ is the global vector of nodal displacements.

The penalized stress tensor for stress evaluation point a then reads

$$\boldsymbol{\sigma}_a(\boldsymbol{x}) = \eta_S(\rho_e(\boldsymbol{x}))\,\hat{\boldsymbol{\sigma}}_a(\boldsymbol{x}). \tag{7}$$

3 Problem formulations

The design variables influence the material properties of the elements and thus the behaviour of the structure, as was discussed in Section 2. They are changed such that the objective function $f(\boldsymbol{x})$ is optimized while the n_c number of functions $g_c(\boldsymbol{x})$ are constrained by the limits $\overline{g}_c$. A general problem formulation reads

$$(\mathbb{P}) \quad \begin{cases} \min\limits_{\boldsymbol{x}} f(\boldsymbol{x}) \\ \text{s.t.} \begin{cases} g_c(\boldsymbol{x}) \leq \overline{g}_c, \ c = 1, .., n_c \\ \epsilon \leq x_e \leq 1, \ e = 1, .., n_e. \end{cases} \end{cases}$$

We use a nested formulation where the displacements are uniquely defined by the design variables and calculated by a standard FE-analysis. An alternative to the nested approach is the simultaneous approach, as described in [25]. In the simultaneous approach, both the displacements $\boldsymbol{u}$ and the design variables $\boldsymbol{x}$ are treated as variables, which are solved for simultaneously and equilibrium is stated as a constraint.

The global stiffness matrix of the structure, $\boldsymbol{K}(\boldsymbol{\rho}(\boldsymbol{x}))$ in (4), is positive definite and thus invertible. Therefore, $\boldsymbol{u}$ can be calculated from the global state equation:

$$\boldsymbol{K}(\boldsymbol{\rho}(\boldsymbol{x}))\,\boldsymbol{u} = \boldsymbol{F}, \tag{8}$$

where $\boldsymbol{F}$ is a vector of external loads. The displacement vector is then a known function of the design variables, given by

$$\boldsymbol{u} = \boldsymbol{u}(\boldsymbol{x}) = \boldsymbol{K}^{-1}(\boldsymbol{\rho}(\boldsymbol{x}))\,\boldsymbol{F}.$$

Traditionally, the objective function in topology optimization has been to minimize the compliance subjected to a constraint on the allowable mass. This formulation reads

$$(\mathbb{P}_{\text{traditional}}) \quad \begin{cases} \min\limits_{\boldsymbol{x}} \dfrac{1}{2}\boldsymbol{F}^T\boldsymbol{u}(\boldsymbol{x}) \\ \text{s.t.} \begin{cases} \sum\limits_{e=1}^{n_e} m_e\rho_e(\boldsymbol{x}) \leq \overline{M} \\ \epsilon \leq x_e \leq 1, \ e = 1, .., n_e, \end{cases} \end{cases}$$

where m_e is the solid element mass of the element related to the e:th design variable and $\overline{M}$ is the total available mass.

The traditional formulation is very popular, much due to its computational efficiency. However, from an engineering point of view it is often more interesting to find the lightest design that has stresses below some stress limit, such as the yield limit, and that is designed so that fatigue failure will not occur. With ($\mathbb{P}_{\text{traditional}}$), several manual test have to be made for different allowable masses and each optimized structure has to be evaluated with respect to e.g. stresses. This manual design iteration can be very time consuming and thus expensive, especially if the optimization and the stress analysis are made by different engineers. Therefore, the stiffness based optimization ($\mathbb{P}_{\text{traditional}}$) is often used to find the optimal load paths rather than to achieve a conceptual design, and it is used only for comparison purpose in this work.

By introducing stress and fatigue constraints in topology optimization, a conceptual design that satisfies, or at least almost satisfies, the stress and fatigue requirements is achieved and the conceptual design is thus closer to a final design. The steps between conceptual design, preliminary design and detailed design are therefore smaller, which will make the product development process faster. Further, the objective function can be to minimize the mass, which means that the lightest design that also satisfies the constraints is achieved without any manual design iterations.

In Paper 1, stress constraints are introduced for different objective functions; the first problem formulation reads

$$(\mathbb{P}_{1a}) \quad \begin{cases} \min\limits_{\boldsymbol{x}} \sum\limits_{e=1}^{n_e} m_e \rho_e(\boldsymbol{x}) \\ \text{s.t.} \begin{cases} \dfrac{\sigma_i^s(\boldsymbol{x})}{\overline{\sigma}^s} \leq 1, \ i = 1, .., n_i \\ \epsilon \leq x_e \leq 1, \ e = 1, .., n_e, \end{cases} \end{cases}$$

where $\sigma_i^s(\boldsymbol{x})$ is the stress measure for stress constraint number i and $\overline{\sigma}^s$ is the static stress limit. As will be discussed in Section 4, we use a clustered approach, where the number of stress constraints n_i will be much lower that the number of design variables n_e.

The stiffness of a structure found by ($\mathbb{P}_{1a}$) might become adequate due to the stress constraints, but there is no guarantee, as was also noticed by Rozvany [39]. If the stiffness is also of importance, a compliance, displacement or eigenfrequency constraint can be added to ($\mathbb{P}_{1a}$). Alternatively, the stress constraints in ($\mathbb{P}_{1a}$) can be added to ($\mathbb{P}_{\text{traditional}}$) in order to achieve the stiffest possible design for a prescribed amount of material, but where also stresses are considered. This formulation will again require manual design iterations in order to find the lowest

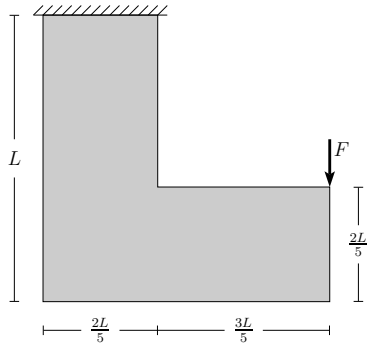

Figure 7: The L-beam problem.

possible mass for which a feasible design is found; the formulation reads

$$(\mathbb{P}_{1b}) \quad \begin{cases} \min\limits_{\boldsymbol{x}} \dfrac{1}{2}\boldsymbol{F}^T\boldsymbol{u}\left(\boldsymbol{x}\right) \\ \text{s.t.} \begin{cases} \dfrac{\sigma_i^s\left(\boldsymbol{x}\right)}{\overline{\sigma}^s} \leq 1, \ i = 1, .., n_i \\ \displaystyle\sum_{e=1}^{n_e} m_e \rho_e\left(\boldsymbol{x}\right) \leq \overline{M} \\ \epsilon \leq x_e \leq 1, \ e = 1, .., n_e. \end{cases} \end{cases}$$

Paper 1 reviews ($\mathbb{P}_{1a}$) and ($\mathbb{P}_{1b}$) and comparisons are also made with ($\mathbb{P}_{\text{traditional}}$). It is found that, compared to the traditional formulation, a different topology is obtained when stress constraints are used and that it is not sufficient to start with a stiffness optimization and then add stress requirements in later design stages.

In order to visualize the differences between the formulations, the L-beam problem, as shown in Figure 7, is solved for the three formulations: ($\mathbb{P}_{\text{traditional}}$), ($\mathbb{P}_{1a}$) and ($\mathbb{P}_{1b}$). The mass obtained for ($\mathbb{P}_{1a}$) is used as mass limit in the two other formulations, so that all designs have the same mass. Particular focus is on removing the internal corner, in order to avoid a stress concentration. The results are shown in Figure 8 and clearly show the differences in design. For ($\mathbb{P}_{1a}$) and ($\mathbb{P}_{1b}$) a radius is created in the internal corner, whereas ($\mathbb{P}_{\text{traditional}}$) creates a singular stress point. More comparisons are made in Paper 1.

Paper 2 introduces fatigue constraints to ($\mathbb{P}_{1a}$), i.e. both static stresses and stresses related to a fatigue analysis are used as constraints. The problem formulation in

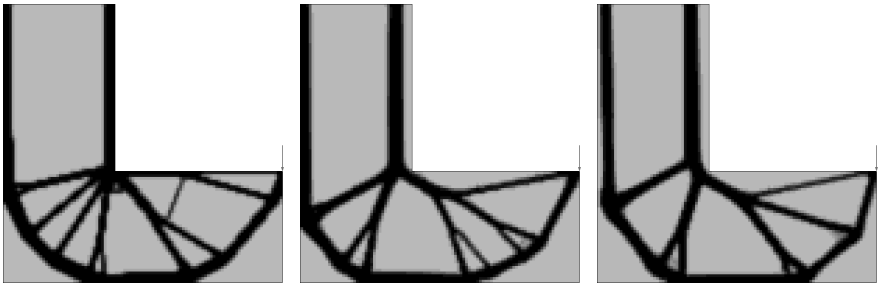

(a) Solution for ($\mathbb{P}_{\text{traditional}}$) (b) Solution for ($\mathbb{P}_{1a}$) (c) Solution for ($\mathbb{P}_{1b}$)

Figure 8: Example of solutions for different problem formulations. The pictures are taken from Paper 1.

Paper 2 reads

$$(\mathbb{P}_2) \quad \begin{cases} \min\limits_{\boldsymbol{x}} \sum\limits_{e=1}^{n_e} m_e \rho_e(\boldsymbol{x}) \\ \text{s.t.} \begin{cases} \dfrac{\sigma_i^s(\boldsymbol{x})}{\overline{\sigma}^s} \leq 1, \ i = 1, .., n_i \\ \dfrac{\sigma_j^f(\boldsymbol{x})}{\overline{\sigma}^f} \leq 1, \ j = 1, .., n_j \\ \epsilon \leq x_e \leq 1, \ e = 1, .., n_e, \end{cases} \end{cases}$$

where the stress measure used for fatigue constraint number j is denoted $\sigma_j^f(\boldsymbol{x})$ and the fatigue stress limit $\overline{\sigma}^f$ is chosen such that the cumulative damage D is below the allowable cumulative damage $\overline{D}$, for prescribed loading conditions during the entire design life. A clustered approach is used also for the fatigue constraints; the number of fatigue constraints n_j is therefore much lower than n_e. Paper 2 also discuss an alternative, more general, formulation of the fatigue constraints, where $D \leq \overline{D}$ is used as constraint directly; further details are discussed in Section 4.2.

4 Constraints adapted for industrial use

4.1 Stress constraints

Stress constraints have been discussed since the very beginning of structural optimization: Dorn et al. [20] used stress constraints in truss optimization in 1964 and in pioneering works on topology optimization by Bendsøe and Kicuchi from 1988 [5] and by Bendsøe from 1989 [3], stress constraints were mentioned, even though it was not used in the optimization. The interest in stress constraints is not surprising as stress is among the most used criterion for engineering purpose.

Since the pioneering works, the compliance based formulation has been synonymous with topology optimization, much due to the added complexity involved with stress constraints. However, stress constraints in topology optimization have been given attention by several authors and the main difficulties that have been associated with stress constraints are:

- Singularity,
- Computational cost due to the large number of constraints.

The singularity problem was first discovered on a truss design by Sved and Ginos [57], where it was found that the stress constraint in a bar is violated when the area of the bar approaches zero, which restraints the bar from being removed. The same applies to 2D and 3D structures. Singularity in optimization problems is discussed by Kirsch [28], Cheng and Jiang [13], Rozvany and Birker [42], Guo and Cheng [24] among others and one way to avoid the singularity problem is the ϵ-approach suggested by Cheng and Guo [14].

The stress penalization method that we use, equation (6), which was also used in [32], originates from Bruggi [8], where it was noted that the stress actually do not need to be proportional to the penalized stiffness. The penalization functions we use, (5) and (6), do not affect the stiffness or stress when the design variable is at its upper bound and they approach zero when the design variable do so. As the reason for introducing the penalization is to end up in a black-and-white design, the stiffness and stress of the optimized design will not be severely influenced by the penalization.

The ϵ-approach was successfully used by Duysinx and Bendsøe [21] and Duysinx

and Sigmund [22], where global and local stress constraints were used, respectively. Local stress constraints imply that one stress constraint is used in each stress evaluation point of each element and global means that one stress constraint is used for the entire model. Local and global stress constraints were also evaluated by Paris et al. [37] and the same authors evaluated a block aggregated approach in [38], where elements were grouped and one stress constraint was applied for each group. A similar approach was made by Le et al. in [32] where a regional stress measure was defined. Our approach relies on the ideas in [38] and [32]; in Paper 1 we develop and evaluate different clustering techniques which, together with a suitable clustered stress measure, are intended to give good representations of the local stresses, despite using a low number of constraints. The clustered stress measure and the clustering techniques are discussed in Section 4.1.1 and Section 4.1.2, respectively.

Another approach to control local stresses with a low number of constraints is suggested by Werme in [60], where stress constraints are used in a maximum stiffness problem. Werme uses an approach with active constraints, i.e. only the design variables related to stresses that in the current iteration are considered to be close enough to their bound are used as constraints. Compared to the local approach, fewer constraints are therefore required, but the method still gives a high number of constraints and rather coarse meshes are used in the examples. Werme defines the active set of constraints as $A(\boldsymbol{x}^l) = \{i \in \{1, ..., n\} | \sigma_i^2(\boldsymbol{x}^l) > \kappa\sigma^{max}\}$, where A is the active set, l is the iteration number, $\sigma_i(\boldsymbol{x})$ is the current local von Mises stress, σ^{max} is the constraint bound and $\kappa > 0$ is the threshold value, e.g. $\kappa = 0.5$. In the paper, a design is generated with topology optimization and the design variable values are then rounded to zero or one. The design is then post-processed using SLIP, as described in [56], which removes unwanted designs such as too thin bars.

Some commercial software, such as Optistruct [36], can handle stress constraints based on a single von Mises measure. However, as mentioned earlier, the global approach is too rough and Optistruct finds a solution for the L-shaped beam in Figure 7 that does not avoid the singularity in the internal corner. For comparison purpose, a topology optimization using ($\mathbb{P}_{1a}$) is made in Optistruct and it is compared to the formulation in this work, which is implemented in TRINITAS [58]. The results are seen in Figure 9 and Table 1. As is seen in the figure, the solution in Optistruct is comparable to a compliance based design, as no radius is created in the internal corner; compare with Figure 8(a). Optistruct was used with default settings, except that a "minimum member size control", i.e. a filter, as described in [62], was added with the same radius as used in TRINITAS. On the one hand, Optistruct finds a solution in a much lower number of iterations and much shorter computational time[1], see the summary in Table 1. On the other hand, the formulation in this work finds a lighter design that also creates a radius in order to avoid the stress concentration in the internal corner. The suggested approach to

[1]The optimizations were performed on different computers, but the two times presented in Table 1 give an estimate of the differences in computational time.

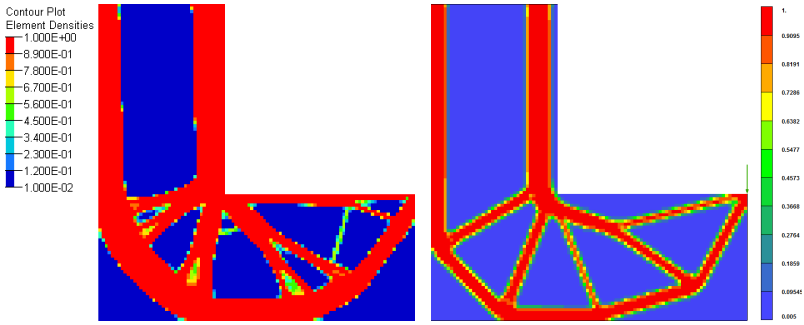

(a) Solution for ($\mathbb{P}_{1a}$) using Optistruct.

(b) Solution for ($\mathbb{P}_{1a}$) using this work, implemented in TRINITAS.

Figure 9: Comparison between commercial software and this work, using three clusters, see also Table 1.

Table 1: Comparison between commercial software and this work, using three clusters, see also Figure 9.

Software	Mass [kg$\times 10^{-3}$]	Number of iterations	Time [minutes]
Optistruct	35.5	34	2
TRINITAS	23.2	500	59

remove the stress concentrations in Optistruct [36] is to continue with local shape optimization. However, in this case, local changes will not be sufficient to reduce the stress concentration and we claim that the total product development time to create a final design will be shorter using the formulation in this work.

4.1.1 Clustered stress measure

Based on the work with global stress constraints in e.g. [21] and from commercial software [36], it is found that the global approach is too rough and generates designs that are very similar to traditional compliance minimization results, see Figure 9(a) and Figure 8(a). This conclusion was also found in the examples in [32]. Topologies that avoid stress concentrations may be obtained with the local approach, but it becomes too expensive for anything else than small test examples.

The clustered approach allows for a trade-off between accuracy and computational cost. The main reason for using clusters is to reduce the n_a number of local constraints (one for each stress evaluation point) to $n_i \ll n_a$ number of clustered constraints (one for each stress cluster) and still maintain the possibility to control the local stresses. We may think of the two extremes: $n_i = 1$ and $n_i = n_a$, which bring us back to the global and local approaches, respectively.

The clustered stress measure we use is a modified P-norm of the local von Mises stresses, even though the method is not restricted to the von Mises criterion. A P-norm has been used in earlier work to group local stresses, [61], [22] and [32], but our modification is different. The local stresses $\sigma_a^{vM}(\boldsymbol{x})$, where a is the stress evaluation point, are raised with the P-norm factor p and summed together with all other points that belong to the current cluster, i. We then divide by the number of stress evaluation point indices N_i that belong to the current set $\Omega_i \subset \Omega$. The clustered stress measure reads

$$\sigma_i^s(\boldsymbol{x}) = \left(\frac{1}{N_i} \sum_{a \in \Omega_i} \left(\sigma_a^{vM}(\boldsymbol{x}) \right)^p \right)^{\frac{1}{p}}. \tag{9}$$

The modification is such that if all the local stresses in a cluster are the same, i.e. $\sigma_a^{vM}(\boldsymbol{x}) = \sigma^{vM}$, we get the desired clustered stress measure

$$\sigma_i^s(\boldsymbol{x}) = \left(\frac{1}{N_i} \sum_{a \in \Omega_i} \left(\sigma_a^{vM}(\boldsymbol{x}) \right)^p \right)^{\frac{1}{p}} = \left(\frac{1}{N_i} \right)^{\frac{1}{p}} \left(N_i \left(\sigma^{vM} \right)^p \right)^{\frac{1}{p}} = \sigma^{vM}. \tag{10}$$

For all other cases, $\sigma_i^s(\boldsymbol{x})$ will underestimate the local stresses, which means that we are not guaranteed (and it is not probable) to have a solution with local stresses below the stress limit. However, higher local stresses can be allowed because the topology optimization is made in a conceptual design phase, where the aim is to find a good structural shape, not to do the final sizing.

The exponent p in (9) has a large influence on what the clustered stress measure represents: $p = 1$ gives the mean stress for each cluster whereas an increasing p brings the clustered stress measure closer to the maximum local stress of each cluster. As shown in [22], the limit value of (9) when p approaches infinity reads

$$\lim_{p \to \infty} \left(\frac{1}{N_i} \sum_{a \in \Omega_i} \left(\sigma_a^{vM}(\boldsymbol{x}) \right)^p \right)^{\frac{1}{p}} = \max_{a \in \Omega_i} \sigma_a^{vM}(\boldsymbol{x}).$$

Due to numerical problems, p should not be too high. Based on numerous test on different test examples and the evaluations in [32] and [22], we use $p = 8$ in Paper 1 and $p = 12$ in Paper 2.

4.1.2 Distribution of points into clusters

The clustered stress measure (9) is greatly influenced by how the clusters are created, i.e. which stress evaluation points that belong to the sets Ω_i, $i = 1, .., n_i$. Two different methods for how the clusters in (9) are created are discussed in Paper 1: the *Stress level* approach and the *Distributed stress* approach.

If the set Ω_i contains stress evaluation points that have similar stress levels, then $\sigma_i^s(\boldsymbol{x})$ will be a good approximation of the local stresses at these stress evaluation

points, as the case shown in (10) is approached. This is exactly what we strive for in the *Stress level* approach, where the clusters are created as follows: all stress evaluation points are sorted in descending order based on the stress level and the first n_a/n_i number of points create the first cluster, the next n_a/n_i points create the second cluster etc. until all n_i number of clusters are filled. We use the same number of points in all clusters, except for the last cluster that might contain fewer points. A variable number of clusters might however be used in future work, where the first cluster, with the highest stresses, could contain a smaller number of points, in order to get an even better control of the highest local stresses. The last clusters, containing low stressed points, will typically have a very low clustered stress measure and will thus not be active in the optimization. The clustering scheme for the *Stress level* approach reads

$$\underbrace{\sigma_1 \geq \sigma_2 \geq \sigma_3 \geq ..... \geq \sigma_{\frac{n_a}{n_i}}}_{\text{cluster } 1} \geq \underbrace{..... \geq \sigma_{\frac{2n_a}{n_i}}}_{\text{cluster } 2} \geq ..... \geq \sigma_{\frac{(n_i-1)n_a}{n_i}} \geq \underbrace{..... \geq \sigma_{n_a}}_{\text{cluster } n_i}.$$

In the *Distributed stress* approach, the stress evaluation points are instead distributed so that each cluster gets approximately the same clustered stress measure, i.e. each cluster is created by high and low stressed points. The motivation for this approach is that a high stress value might be damped by a presumable large number of low stressed points that it is clustered with. Therefore, convergence may be simplified. The clustering scheme for the *Distributed stress* approach reads

$$\underbrace{\sigma_1}_{\text{cluster } 1} \geq \underbrace{\sigma_2}_{\text{cluster } 2} \geq ..... \geq \underbrace{\sigma_{\frac{n_a}{n_i}-1}}_{\text{cluster } (n_i-1)} \geq \underbrace{\sigma_{\frac{n_a}{n_i}}}_{\text{cluster } n_i} \geq \underbrace{\sigma_{\frac{n_a}{n_i}+1}}_{\text{cluster } 1} \geq ..... \underbrace{\geq \sigma_{n_a}}_{\text{cluster } n_i}.$$

4.1.3 Periodic reclustering

Another important issue regarding the clustering is that the clusters may have to be updated periodically. For example, if the clusters are created based on the stresses of the initial design, then, after a few iterations, the points are no longer sorted into the clusters in the way they were intended to. When this reclustering is made, the problem is slightly changed as the clustered stress measure is calculated based on another set of points than in the previous iteration. The two clustering techniques as well as the influence of the reclustering frequency are evaluated in Paper 1.

4.2 Fatigue constraints

Fatigue constrained topology optimization is a research area that previously has been almost unexplored, much due to the problems that occur for stress constraints. Structural optimization in general has however been used to find designs that fulfil

fatigue life aspects in a number of works. For example, Kaya et al. [27] investigated a failed clutch fork and used compliance based topology optimization, followed by response surface based shape optimization, in order to achieve a design with a lower von Mises stress. The fatigue analysis was made with a constant amplitude load curve and the software MSC Fatigue [49]. Mrzyglod and Zielinski [34] used Dang Van's criterion to formulate a multiaxial high-cycle fatigue constraint in a shape optimization of a suspension arm. The authors evaluated different criteria in [35] and discussed the implementation in [33]. The fatigue analysis software FEMFAT was integrated into the optimization software TOSCA from FE-design [23] in [29], where shape and topology optimization was made with fatigue considerations. In [18], the fatigue life was maximized in a 3D topology optimization problem, considering elasto-plastic low-cycle fatigue. Optistruct [36] also has an integrated fatigue analysis software and can have fatigue constraints in topology optimization. However, based to the performance of the stress constraint shown in Figure 9, the method is expected to be too rough.

Paper 2 introduces high-cycle fatigue constraints that are based on the highest tensile principal stresses. The material data used in the fatigue analysis is based on uniaxial fatigue tests; therefore, the highest principal stresses correspond better to the material data than what e.g. stresses according to the von Mises criterion do. The tensile stresses have a much higher influence on the fatigue life than compressive stresses, which is the reason why only tensile stresses are considered. The fatigue analysis is made with an in-house code from Saab AB [1] and it is used as a tool to find a structure that can endure repeated loading conditions without failure. No attention is therefore given to mechanisms behind the fatigue phenomenon, such as material aspects, the influence of different load ratios etc.

We focus on structural parts on a military aircraft, for which fatigue life is often expressed in terms of *flight hours*. The aircraft is designed for a specific number of flight hours; therefore, structural optimization can be used to design the part such that fatigue will not occur during the specific finite life, or before predetermined service intervals. That is, a so-called *Safe-Life* approach is used.

The aim of the fatigue constraints is not to replace a final fatigue analysis, but to find a conceptual design that with the least possible changes can be changed into a final design, for which fatigue failure will not occur. In order to decrease the number of fatigue constraints, the same approach as for the static stress constraints is used: stress evaluation points are clustered using the *Stress level* approach and the clusters are updated every iteration. Clustered stress measures $\sigma_j^f(\boldsymbol{x})$ are calculated by (9), but where the local stresses are the highest tensile principal stresses, instead of the von Mises stresses. One fatigue constraint is then applied to each cluster, rather than to every stress evaluation point. The fatigue analysis is very sensitive to the stress; it is thus contradictory to use the clustered approach as we know that local stresses will be higher. Further, the finite element mesh and the element type that is used in the topology optimization may not be adequate for fatigue analysis. However, the clustered approach is a necessity to be able

to solve anything but very small problems and the mesh is sufficient in terms of obtaining optimized designs that are free from large stress concentrations and that are dimensioned with respect to the critical fatigue stress.

4.2.1 Load spectrum and material data

A local load spectrum, that describes the variation of the applied load, has to be available for the fatigue analysis. The local load spectrum can be determined from a global spectrum, e.g. by the use of a global FE-model, where the global spectrum describes all the missions the aircraft is intended to fulfil during its entire life. Each mission, which for a fighter aircraft can be for example training, combat or show, is usually flown a large number of times and the loads for the manoeuvres in the missions are estimated. The loads are measured during flight using accelerometers and strain gauges, which increase the confidence in the load spectrum, but in an early design phase of an aircraft project, when mass and stiffness of the aircraft are not completely known, the load spectrum will contain uncertainties.

In this work we do not consider how the loads are determined, we assume that the loads are known and that load pairs have been identified from peak and trough values, using some cycle counting method, such as Rainflow count [52], [17]. Figure 10 shows an example of a load spectrum, where load pairs have been identified. It specifies a load factor f of the mass m and gives the number of cycles n of each load pair. The corresponding load at each load level is $F = mgf$.

The allowable number of cycles are determined from Wöhler- or Haigh diagrams, which are based on numerous fatigue tests made on polished test specimens. A Wöhler diagram describes the number of cycles to fatigue failure as a function of the stress amplitude, for a constant load ratio $R = F_{min}/F_{max}$. If the load ratio is altered, a Haigh diagram is achieved; it describes the relationship between the mean stress and the stress amplitude for a specific number of cycles. Thus, it represents a series of Wöhler diagrams, as shown in Figure 11. Reduction of the diagrams is discussed in Section 4.2.3.

4.2.2 Fatigue analysis

The fatigue methodology in Paper 2 is a traditional high-cycle fatigue methodology, where the damage for each load pair in a given load spectrum is accumulated by Palmgren-Miner's rule. No distinction is made between crack initiation, crack propagation and fatigue failure; detailed descriptions of the methodology are given by Suresh [52] or Dahlberg and Ekberg [17].

We only consider materials that are in a linear elastic region. A unit load F_{unit} is therefore used in the FE-analysis and the corresponding stress $\sigma_{\text{unit}}(\boldsymbol{x})$ is scaled according to the load levels in the load spectrum. We express the FE-analysis as

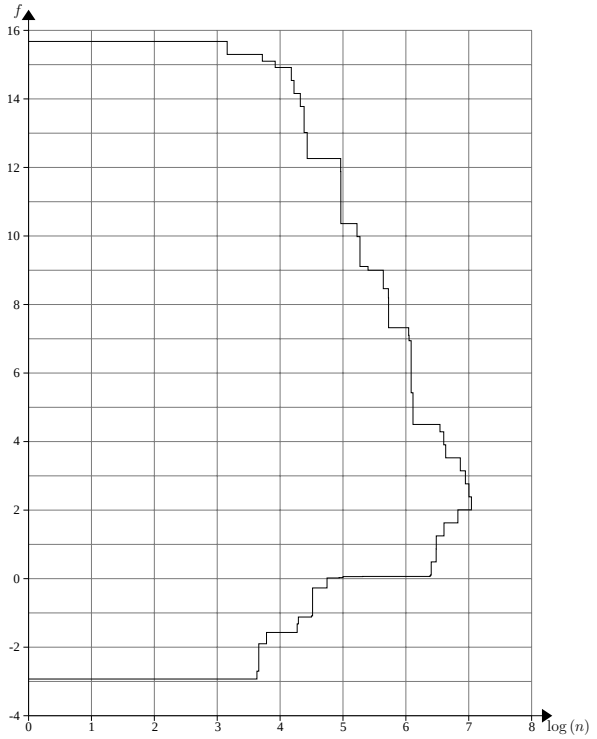

Figure 10: Load spectrum representing the load factor n on the ordinate and the logarithm of the number of cycles n on the abscissa.

an operator $\mathbb{FE}$ that maps a design $\boldsymbol{x}$ and the unit load to a corresponding stress, that is

$$\sigma_{\text{unit}}(\boldsymbol{x}) = \mathbb{FE}(F_{\text{unit}}, \boldsymbol{x}). \tag{11}$$

For each load pair l, the corresponding mean stress $\sigma_l^{\text{mean}}(\boldsymbol{x})$ and amplitude stress $\sigma_l^{\text{amp}}(\boldsymbol{x})$ are determined by operators $\mathbb{S}_l$, such that

$$(\sigma_l^{\text{mean}}(\boldsymbol{x}), \sigma_l^{\text{amp}}(\boldsymbol{x})) = \mathbb{S}_l(\sigma_{\text{unit}}(\boldsymbol{x})). \tag{12}$$

The allowable number of cycles for each load pair N_l is then determined from the Haigh diagram by operators $\mathbb{H}_l$, as

$$N_l = \mathbb{H}_l(\sigma_l^{\text{mean}}(\boldsymbol{x}), \sigma_l^{\text{amp}}(\boldsymbol{x})) = \mathbb{H}_l(\mathbb{S}_l(\sigma_{\text{unit}}(\boldsymbol{x}))). \tag{13}$$

The cumulative damage $D(\sigma_{\text{unit}}(\boldsymbol{x}))$ is determined according to Palmgren-Miner's rule, by comparing the actual number of cycles n_l, given by the load spectrum, with the allowable number of cycles for all L load pairs in the spectrum. Palmgren-

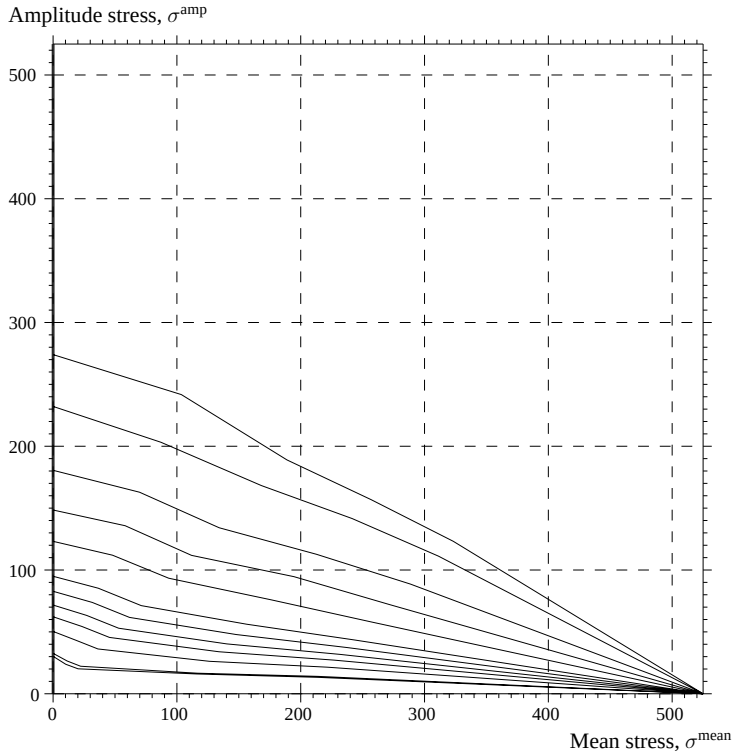

Figure 11: Haigh diagram, the curves represents constant life, i.e. different N.

Miner's rule reads

$$D\left(\sigma_{\text{unit}}\left(\boldsymbol{x}\right)\right) = \sum_{l=1}^{L} \frac{n_l}{N_l} = \sum_{l=1}^{L} \frac{n_l}{\mathbb{H}_l\left(\mathbb{S}_l\left(\sigma_{\text{unit}}\left(\boldsymbol{x}\right)\right)\right)}. \tag{14}$$

and fatigue failure is expected to occur if $D \leq \overline{D} \leq 1$.

Usually, when a given structure is analysed, there are a relatively low number of critical spots that need to be analysed with respect to fatigue. This is not the case in topology optimization where the design is achieved iteratively. Therefore, all points need to be constrained and in this work the stress response in (11) is replaced by the clustered stress measures $\sigma_j^f\left(\boldsymbol{x}\right)$.

4.2.3 Fatigue data

Several factors influence the local resistance to crack initiation for a structural part. The loading conditions, the local stresses and material properties are perhaps

the most obvious and these are also the factors that have the highest influence. However, the local stresses might be affected by stress concentrations, which also have a prominent effect on the fatigue life. If a certain stress occurs in a point with a stress concentration, the damage for that stress is smaller than if the same stress would occur in a point without a stress concentration. This is because the volume affected by the high stress is smaller if it occurred at a stress concentration, and the probability that a material defect exists in that volume is thus smaller. With the same argument, the volume affected by a certain stress compared to the volume of the test specimen has an influence on the expected life.

Fatigue crack initiation is a surface phenomenon. The highest stresses often occur at the surface, which in combination with a surface roughness due to machining operations, surface treatments and environmental ware makes the surface more prone to crack initiation. These factors also have to be considered in the fatigue analysis and are so by reduction factors that reduce the allowable number of cycles in the Wöhler and Haigh diagrams. The diagrams are constructed such that the probability of failure, based on data from the test specimens, should be below a certain percentage. The reductions are then made in order to make the diagrams valid for the specific point of interest, rather than for the test specimen. The diagram is also reduced with respect to the risk of scatter in the material.

In the topology optimization, the fatigue analysis has to be simplified and the factors are consequently not considered as variables, but are specified prior to the optimization and then considered as constant, so that the fatigue constraints are only dependent on the stress. The surface roughness and the surface treatment are likely to be the same for the entire structure, as well as the environment it will operate in. The factor that is the hardest to estimate, which unfortunately also has a high influence on the fatigue life, is the stress concentration. Notched test specimens are used to create Haigh diagrams for different K_t-factors. The stress from the FE-analysis should then be divided by the K_t-factor, to get a theoretical nominal stress, which is then used with the correct Haigh diagram. This implies that different diagrams should be used for different points on the structure. However, in topology optimization, where all points contribute to a fatigue constraint, it is desirable to use the same diagram for the entire structure. A simplified approach is therefore used; it is assumed that the stresses from the FE-analysis belong to points where there is a small stress concentration. The material data for this assumed K_t-factor is then used for the entire structure. Fatigue failure most often occurs in a high stress concentration; therefore, fatigue failure is assumed to be less likely to occur than what we calculate. In Paper 2 we use $K_t = 1.5$, experience in future work is required to find out just how rough this estimation is. If it is too conservative, the fatigue life will be underestimated, which will result in heavy structures. If it is not conservative enough, the optimization will find structures with low mass that will not satisfy the fatigue life in later design phases.

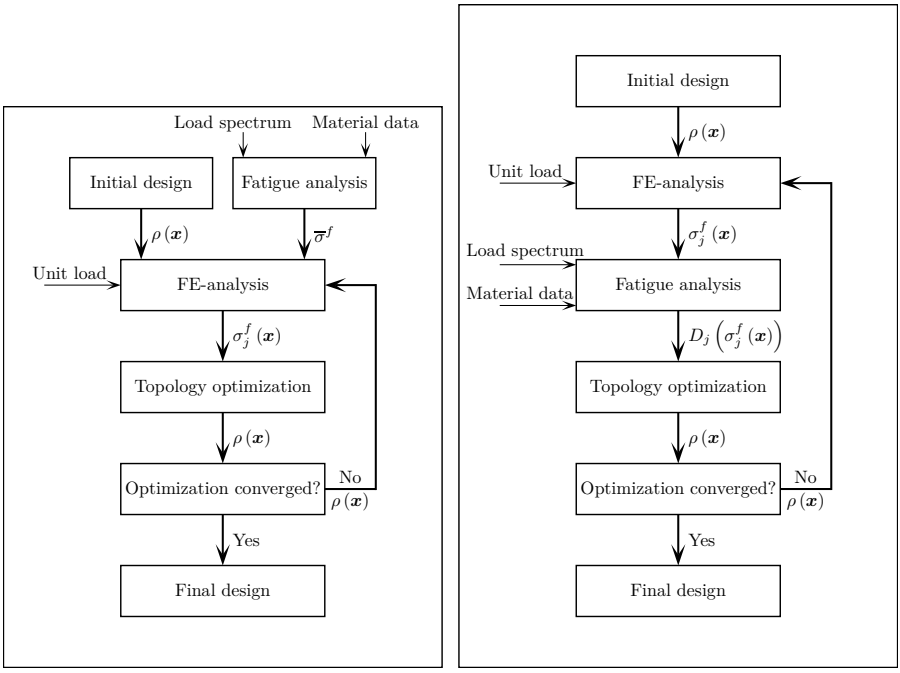

(a) Flow scheme for fatigue constraints in ($\mathbb{P}_2$). (b) Alternative flow scheme.

Figure 12: Flow schemes corresponding to the two presented approaches to fatigue constraints.

4.2.4 Formulation of the fatigue constraints

In paper 2 we introduce two approaches towards fatigue constraints; both approaches are based on that the part is designed for a specific life time, which is used to determine a fatigue criterion.

In the first approach, the cumulative damage, (14), is used as constraint. Thus, in every iteration, the fatigue calculation is made once for each fatigue constraint, in order to determine the cumulative damages $D_j\left(\sigma_j^f(\boldsymbol{x})\right)$. The flow scheme is visualized in Figure 12(b). This approach can be used if some factor is updated in the optimization, for example if some estimate of local K_t-factors should be used in future work.

In the second approach, all factors discussed in Section 4.2.3 are fixed, so the design dependence is removed from the fatigue analysis, i.e. from (12)-(14). Therefore, the fatigue analysis can be separated from the optimization problem. Thus, the critical fatigue stress $\overline{\sigma}^f$, which is the highest stress that gives an allowable cumulative damage, can be determined in advance and then used as constraint limit in the topology optimization problem ($\mathbb{P}_2$). The flow scheme is shown in Figure 12(a) and

the critical fatigue stress is found by solving the following problem:

$$(\mathbb{P}_{\text{crit}}) \quad \begin{cases} \max\limits_{\overline{\sigma}^f} \ \overline{\sigma}^f \\ \text{s.t.} \begin{cases} \displaystyle\sum_{l=1}^{L} \frac{n_l}{\mathbb{H}_l\left(\mathbb{S}_l\left(\overline{\sigma}^f\right)\right)} \leq \overline{D}. \end{cases} \end{cases}$$

Note that the two approaches solve the exact same problem as long as no factors are updated. However, the second approach is used in Paper 2 because no factors are updated and as the fatigue software does not need to be implemented into the FE and optimization code for this approach.

5 Solving the optimization problem

5.1 Sensitivity analysis

Sensitivity analysis is a central part in topology optimization as the mathematical programming algorithms are based on sensitivity information. As a note, there exist non-gradient based topology optimization methods; however, motivated by the critical review by Sigmund [47], these methods are not discussed in this work.

Depending on the type of problem to be solved, two different approaches are used for the sensitivity analysis: the direct and the adjoint method, [2], [15]. The latter is preferable when there are more design variables than constraints, which is usually the case in topology optimization.

In structural optimization the objective function and the constraint functions are often dependent on the displacements, i.e. $f(\boldsymbol{x}, \boldsymbol{u}(\boldsymbol{x}))$ and $g_c(\boldsymbol{x}, \boldsymbol{u}(\boldsymbol{x}))$. Using the chain rule, we get the sensitivity of the constraints in the general problem formulation ($\mathbb{P}$), as

$$\frac{\partial g_c(\boldsymbol{x}, \boldsymbol{u}(\boldsymbol{x}))}{\partial x_b} = \frac{\partial g_c(\boldsymbol{x}, \boldsymbol{u}(\boldsymbol{x}))}{\partial x_b} + \frac{\partial g_c(\boldsymbol{x}, \boldsymbol{u}(\boldsymbol{x}))}{\partial \boldsymbol{u}(\boldsymbol{x})} \frac{\partial \boldsymbol{u}(\boldsymbol{x})}{\partial x_b}, \tag{15}$$

where the sensitivity of the displacements is required. This is calculated from the equilibrium equation (8), here expressed as

$$\boldsymbol{K}(\boldsymbol{x})\,\boldsymbol{u}(\boldsymbol{x}) = \boldsymbol{F}(\boldsymbol{x}),$$

with the derivative

$$\frac{\partial \boldsymbol{K}(\boldsymbol{x})}{\partial x_b}\boldsymbol{u}(\boldsymbol{x}) + \boldsymbol{K}(\boldsymbol{x}) \frac{\partial \boldsymbol{u}(\boldsymbol{x})}{\partial x_b} = \frac{\partial \boldsymbol{F}(\boldsymbol{x})}{\partial x_b}.$$

By rearranging we find that the displacement sensitivity reads

$$\frac{\partial \boldsymbol{u}(\boldsymbol{x})}{\partial x_b} = \boldsymbol{K}^{-1}(\boldsymbol{x}) \left[\frac{\partial \boldsymbol{F}(\boldsymbol{x})}{\partial x_b} - \frac{\partial \boldsymbol{K}(\boldsymbol{x})}{\partial x_b}\boldsymbol{u}(\boldsymbol{x}) \right], \tag{16}$$

which is now inserted into (15):

$$\frac{\partial g_c(\boldsymbol{x}, \boldsymbol{u}(\boldsymbol{x}))}{\partial x_b} = \frac{\partial g_c(\boldsymbol{x}, \boldsymbol{u}(\boldsymbol{x}))}{\partial x_b} + \frac{\partial g_c(\boldsymbol{x}, \boldsymbol{u}(\boldsymbol{x}))}{\partial \boldsymbol{u}(\boldsymbol{x})} \boldsymbol{K}^{-1}(\boldsymbol{x}) \left[\frac{\partial \boldsymbol{F}(\boldsymbol{x})}{\partial x_b} - \frac{\partial \boldsymbol{K}(\boldsymbol{x})}{\partial x_b}\boldsymbol{u}(\boldsymbol{x}) \right]. \tag{17}$$

From here on the two methods differ: in the direct method, (16) is solved once for each design variable and the result is inserted into (15) once for each b. In the adjoint method, an adjoint variable vector $\boldsymbol{\lambda}_c$ is defined as

$$\boldsymbol{\lambda}_c = \left(\frac{\partial g_c\left(\boldsymbol{x}, \boldsymbol{u}\left(\boldsymbol{x}\right)\right)}{\partial \boldsymbol{u}\left(\boldsymbol{x}\right)} \boldsymbol{K}^{-1}\left(\boldsymbol{x}\right) \right)^T = \boldsymbol{K}^{-T}\left(\boldsymbol{x}\right) \left(\frac{\partial g_c\left(\boldsymbol{x}, \boldsymbol{u}\left(\boldsymbol{x}\right)\right)}{\partial \boldsymbol{u}\left(\boldsymbol{x}\right)} \right)^T. \tag{18}$$

Inserting $\boldsymbol{\lambda}_c$ into (17) yields

$$\frac{\partial g_c\left(\boldsymbol{x}, \boldsymbol{u}\left(\boldsymbol{x}\right)\right)}{\partial x_b} = \frac{\partial g_c\left(\boldsymbol{x}, \boldsymbol{u}\left(\boldsymbol{x}\right)\right)}{\partial x_b} + \boldsymbol{\lambda}_c^T \left[\frac{\partial \boldsymbol{F}\left(\boldsymbol{x}\right)}{\partial x_b} - \frac{\partial \boldsymbol{K}\left(\boldsymbol{x}\right)}{\partial x_b} \boldsymbol{u}\left(\boldsymbol{x}\right) \right]. \tag{19}$$

In the adjoint method (18) has to be solved for each constraint and each $\boldsymbol{\lambda}_c$ is then inserted into (19).

The sensitivity analysis of the stress and fatigue constraints in Section 4.1 and Section 4.2 are derived in Paper 1 and Paper 2, respectively.

5.2 The method of moving asymptotes, MMA

The Method of Moving Asymptotes, MMA, developed by Svanberg 1987 [53] is among the most used algorithms for solving topology optimization problems. MMA creates subproblems that approximate the original problem at the current design. The subproblems are chosen such that they are separable and convex, i.e. there is always an optimal point for the subproblems and they are easily solved.

MMA uses the current and previous design variable values in order to determine if the convergence is smooth or oscillating, upon which the solver modifies the allowable design variable changes, so that the solver is more conservative or allows for faster convergence. The allowable changes are determined by vertical asymptotes which are updated in each iteration and chosen, for each $e = 1, .., n_e$, such that $L_e^k < x_e^k < U_e^k$, where k denotes the current iteration and L_e and U_e are the lower and the upper asymptotes, respectively. MMA has its roots in CONLIN, which is obtained as a special case if the asymptotes are chosen as $L_e = 0$ and $U_e \to \infty$. For $k \geq 2$, the asymptotes are updated as

$$\begin{aligned} L_e^k &= x_e^k - \gamma_e^k \left(x_e^{k-1} - L_e^{k-1} \right) \\ U_e^k &= x_e^k - \gamma_e^k \left(U_e^{k-1} - x_e^{k-1} \right), \end{aligned}$$

where γ_e^k is specified in [54] and [55] as

$$\gamma_e^k = \begin{cases} 0.7 & \text{if } \left(x_e^k - x_e^{k-1} \right) \left(x_e^{k-1} - x_e^{k-2} \right) < 0, \\ 1.2 & \text{if } \left(x_e^k - x_e^{k-1} \right) \left(x_e^{k-1} - x_e^{k-2} \right) > 0, \\ 1 & \text{if } \left(x_e^k - x_e^{k-1} \right) \left(x_e^{k-1} - x_e^{k-2} \right) = 0. \end{cases}$$

In this work, the suggested value on the widening of γ_j^k has been narrowed in order to achieve a more conservative setting of the solver. Instead of 1.2, values between $0.05 - 1.1$ are used in Paper 1 and 1.08 is used in Paper 2.

Another popular algorithm is the optimality criteria (OC) method, which is used extensively in the literature for solving ($\mathbb{P}_{\text{traditional}}$). The development of the method can be traced back to the 1960s and it has been used since the 1970s, see [2] for historical details. The OC method is simpler than MMA and uses a fixed move limit, but the method gives fast convergence for ($\mathbb{P}_{\text{traditional}}$).

6 Future work

6.1 Higher order elements and three dimensional problems

Four-node bilinear elements are usually used in topology optimization problems, much due to their simplicity and low computational cost. However, the bilinear elements have a number of drawbacks, [16], e.g. parasitic shear, i.e. when exposed to pure bending they display not only bending strain, but also shear strain, which gives the elements a stiffer behaviour. This behaviour is avoided for 2D problems if eight-node Serendipity or nine-node Lagrangian elements are used instead.

The extension into three dimensional problems is necessary in order to use topology optimization for industrial applications. Only a very limited number of problems can be simplified to the 2D plane stress assumption that we have discussed so far. Therefore, both papers in this thesis are formulated in a general manner, so that they apply to elements with several stress evaluation points as well as 3D problems. However, the current implementation does not yet fully support this and only 2D problems with bilinear elements have been solved in the current work.

6.2 Fatigue constraints only on the boundaries

Fatigue failure is due to an initiated crack that has propagated until the remaining structure becomes too weak and a fracture occurs. Crack initiation is a phenomenon that usually occurs at the surface, as the surface is subjected to environmental ware, might have a rough finish and as the highest stresses often occur at the surface. There are some exceptions, e.g. welds and casts, but those are usually avoided in the avionic industry and are consequently not considered in this work. It is thus sufficient to consider the boundaries of a structure while evaluating fatigue critical points. A stress state considered for fatigue in a 3D structure is thus biaxial and in a 2D structure it can be considered as uniaxial.

When formulating the fatigue constraints, the fact that fatigue is a surface phenomenon can be used; only the elements that in the current iteration are close to a boundary may therefore be subjected to fatigue constraints. A visualization is shown in Figure 13, where the circles represent the filter radius. This will allow

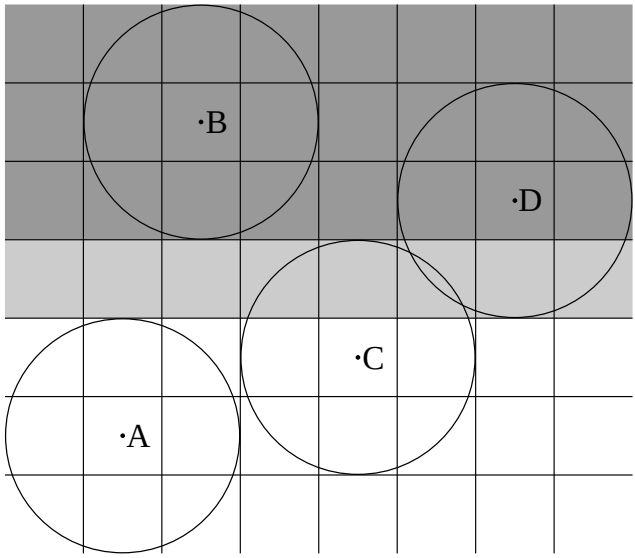

Figure 13: Subset of the FE-mesh. Dark grey=structural member, white=void, bright grey=intermediate value. Elements A and B will not be subjected to fatigue constraints. Elements C and D are close to a boundary and will have fatigue constraints.

for fewer fatigue constraints and thus shorter computational time, or alternatively, fewer members may be related to a fixed number of fatigue constraints, meaning that the clustered stress measures will be better approximations of the considered local stresses. However, the boundaries in the topology optimization are not well defined, as they are blurred due to the filter and as they might move and change shape between iterations.

Using the filter we suggest a simple, but efficient, way to identify elements that in the current iteration are surrounded by solid or void elements, i.e. that do not belong to a boundary and thus will not be subjected to fatigue constraints. The basic idea is that an element is not located at a boundary if it is totally surrounded by elements with the same design variable value as its own. If we look at the design variable filter in (3), we realize that this information already exists and it is simply when $\rho_e(\boldsymbol{x}) = x_e$.

When all design variables inside design variable x_e's filter radius are equal to x_e, we have

$$\rho_e(\boldsymbol{x}) = \frac{\sum\limits_{k\in\Omega_e} w_k x_k}{\sum\limits_{k\in\Omega_e} w_k} = x_e \frac{\sum\limits_{k\in\Omega_e} w_k}{\sum\limits_{k\in\Omega_e} w_k} = x_e. \tag{20}$$

Thus, the fatigue constraint may be removed from elements where $\rho_e(\boldsymbol{x}) = 1$ or

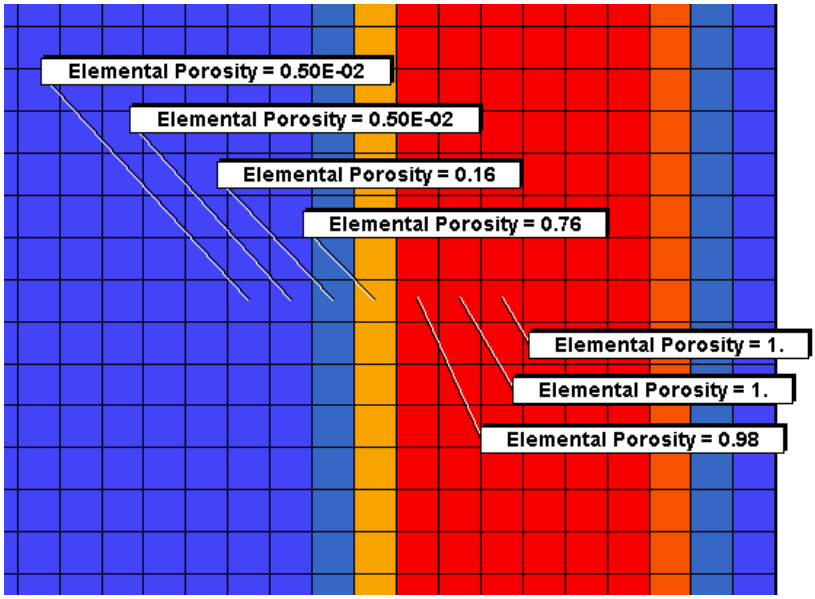

Figure 14: Variation of the design variable values

$\rho_e(\boldsymbol{x}) = \epsilon$ and $|\rho_e(\boldsymbol{x}) - x_e| < \xi$, where ξ is a small positive value that allows for some numerical tolerance. If a boundary is changed in the next iteration, other elements may be subjected to a fatigue constraint.

Figure 14 shows a subset of the finite element mesh in an optimized design, where some design variable values are displayed. The filter uses a radius of 1.5×element length, i.e. the two vertical and the two horizontal neighbouring design variables contribute to $\rho_e(\boldsymbol{x})$. Looking at a horizontal row of elements, we find that only five of the displayed elements along the horizontal would be identified as close to the boundary and fatigue constraints would therefore only be applied to the five respective elements.

6.3 Removal and reintroduction of design variables

The idea presented in Section 6.2 can also be used to remove design variables from the optimization problem, in order to decrease the computational cost. As the connectivity change during iterations, design variables may be removed if $\rho_e(\boldsymbol{x}) = 1$ or $\rho_e(\boldsymbol{x}) = \epsilon$ and $|\rho_e(\boldsymbol{x}) - x_e| < \xi$, and a removed design variable may be reintroduced if $|\rho_e(\boldsymbol{x}) - x_e| \geq \xi$. The gain in efficiency, i.e. reduction of computational cost, will be achieved first when solid and void areas are created and the computational cost will decrease as the solution converges towards a black-and-white solution.

New structural members most often develop from areas with intermediate design variable values or as branches from solid areas and not from voids since the structural response in such areas is weak. With this removal and reintroduction method, new structural members can arise through a void between solid members, but it will take several iterations more than regularly as the design variables have to become active before they can change.

A somewhat similar approach, using the filter, was proposed by Bruns and Tortorelli in [12], where elements whose respective design variable approached their lower bound were removed from the structural analysis and sensitivity analysis, if the design variables within its filter radius also had reached the lower bound.

6.4 Actual risk of fatigue failure

As a last remark and opening for future work, a short discussion is made regarding the actual risk of fatigue failure. The fatigue analysis is probability based, where material data is created such that fatigue will not occur within a certain probability. A structural optimization with fatigue constraints strives for a design where every point on the structural part is at the fatigue limit. The probability of failure will therefore be higher in an optimized part, compared to a manually designed part, where there are often a very limited number of points that might be critical for fatigue. Thus, for a complete aircraft, where many structural parts have been optimized, the probability of failure is further increased and the total probability for a complete fleet of aircrafts will need to be constrained. Therefore, suitable safety factors have to be considered in order to keep the total probability of failure at an allowable limit.

7 Conclusions

This work presents a step towards more advanced topology optimizations in a conceptual design stage. The main objective has been to generate light weight structures that are well prepared for the requirements, in this case stress and fatigue, that are used in industrial applications. The designs obtained in this work are appealing in the sense that large stress concentrations are avoided and as the structural shapes are simple. However, an extension to three dimensional problems in future work is required in order to evaluate the methods for industrial applications.

The clustered approach that has been developed gives a trade-off between computational cost and accuracy and has during the work proven to work well. The computational cost is considerably higher than for the traditional stiffness based problem formulation, but as the designs obtained in this work are more mature, the total product development time is expected to be shorter.

8 Review of included papers

Paper I

Stress constrained topology optimization

In the first paper, static stress constraints based on von Mises stress criterion are introduced in topology optimization problems, where the mass is minimized or the stiffness is maximized. The main focus is on how to formulate the stress constraints such that the computational cost is reasonable, while a good representation of the local stresses is maintained. This is achieved by dividing the stress evaluation points into clusters, where a clustered stress measure is calculated. One stress constraint is then applied to each cluster instead of each stress evaluation point, which greatly reduces the number of constraints. Two different methods for sorting the stress evaluation points into the different clusters are evaluated as well as the question whether the clusters should be fixed or updated during the iterations. Two different examples are used to confirm the analytically discussed differences between the methods and problem formulations.

Paper II

Fatigue constrained topology optimization

The second paper addresses topology optimization of structures subjected to repeated loading conditions, where a fatigue failure might occur even if the stresses are below the yield limit of the material. Fatigue constraints are introduced in order to find a light weight design that is dimensioned by the critical fatigue stress and that avoids stress concentrations. A fatigue analysis software is used to determine the highest stress that gives an allowable cumulative damage for prescribed loading conditions during a specific life time. The highest tensile principal stress is used as fatigue stress measure in the optimization and the fatigue constraints are used together with the von Mises based static stress constraints developed in Paper 1. For comparison purposes, the difference between stress constraints based on von Mises and the highest tensile principal stress are also evaluated.

Bibliography

[1] Saab AB. http://www.saabgroup.com.

[2] Martin Philip Bendsøe and Ole Sigmund. *Topology Optimization - Theory, Methods, and Applications*. Springer Verlag, Berlin, second edition edition, 2003.

[3] M.P. Bendsøe. Optimal shape design as a material distribution problem. *Structural optimization*, 1(4):193–202, 1989.

[4] M.P. Bendsøe, A. Ben-Tal, and J. Zowe. Optimization methods for truss geometry and topology design. *Structural and Multidisciplinary Optimization*, 7(3):141–159, 1994.

[5] M.P. Bendsøe and N. Kikuchi. Generating optimal topologies in structural design using a homogenization method. *Computer methods in applied mechanics and engineering*, 71(2):197–224, 1988.

[6] M.P. Bendsøe and O. Sigmund. Material interpolation schemes in topology optimization. *Archive of Applied Mechanics*, 69(9):635–654, 1999.

[7] T. Borrvall and J. Petersson. Topology optimization using regularized intermediate density control. *Computer Methods in Applied Mechanics and Engineering*, 190(37):4911–4928, 2001.

[8] M. Bruggi. On an alternative approach to stress constraints relaxation in topology optimization. *Structural and multidisciplinary optimization*, 36(2):125–141, 2008.

[9] TE Bruns. A reevaluation of the simp method with filtering and an alternative formulation for solid–void topology optimization. *Structural and Multidisciplinary Optimization*, 30(6):428–436, 2005.

[10] TE Bruns. Zero density lower bounds in topology optimization. *Computer methods in applied mechanics and engineering*, 196(1-3):566–578, 2006.

[11] T.E. Bruns and D.A. Tortorelli. Topology optimization of non-linear elastic structures and compliant mechanisms. *Computer Methods in Applied Mechanics and Engineering*, 190(26-27):3443–3459, 2001.

[12] TE Bruns and DA Tortorelli. An element removal and reintroduction strategy

for the topology optimization of structures and compliant mechanisms. *International journal for numerical methods in engineering*, 57(10):1413–1430, 2003.

[13] G. Cheng and Z. Jiang. Study on topology optimization with stress constraints. *Engineering Optimization*, 20(2):129–148, 1992.

[14] GD Cheng and X. Guo. ε-relaxed approach in structural topology optimization. *Structural and Multidisciplinary Optimization*, 13(4):258–266, 1997.

[15] P.W. Christensen and A. Klarbring. *An introduction to structural optimization*, volume 153. Springer Verlag, 2008.

[16] RD Cook, DS Malkus, ME Plesha, and RJ Witt. *Concepts and applications of finite element analysis*. John Wiley & Sons, 2002.

[17] T. Dahlberg and A. Ekberg. *Failure, fracture, fatigue: an introduction*. Studentlitteratur, 2002.

[18] B. Desmorat and R. Desmorat. Topology optimization in damage governed low cycle fatigue. *Comptes Rendus Mecanique*, 336(5):448–453, 2008.

[19] A. Diaz and O. Sigmund. Checkerboard patterns in layout optimization. *Structural and Multidisciplinary Optimization*, 10(1):40–45, 1995.

[20] W.S. Dorn, R.E. Gomory, and H.J. Greenberg. Automatic design of optimal structures. *Journal de mecanique*, 3(6):25–52, 1964.

[21] P. Duysinx and M.P. Bendsøe. Topology optimization of continuum structures with local stress constraints. *International Journal for Numerical Methods in Engineering*, 43(8):1453–1478, 1998.

[22] P. Duysinx and O. Sigmund. New developments in handling stress constraints in optimal material distribution. *American institute of aeronautics and astronautics*, 4906:1501–1509, 1998.

[23] FE-Design. Tosca, 2012. http://www.fe-design.com/.

[24] X. Guo, G. Cheng, and K. Yamazaki. A new approach for the solution of singular optima in truss topology optimization with stress and local buckling constraints. *Structural and Multidisciplinary Optimization*, 22(5):364–373, 2001.

[25] R.T. Haftka. Simultaneous analysis and design. *AIAA journal*, 23(7):1099–1103, 1985.

[26] T.J.R. Hughes. *The finite element method: linear static and dynamic finite element analysis*. Prentice-hall, 1987.

[27] N. Kaya, İ. Karen, and F. Öztürk. Re-design of a failed clutch fork using topology and shape optimisation by the response surface method. *Materials & Design*, 31(6):3008–3014, 2010.

[28] U. Kirsch. On singular topologies in optimum structural design. *Structural and Multidisciplinary Optimization*, 2(3):133–142, 1990.

[29] Gruen Florian Eichlseder Wilfried Puchner Klaus. Shape- and topology optimization regarding fatigue analysis. In *Cumulative Fatigue Damage, Seville (Spain)*, 2003.

[30] M. Kočvara. Topology optimization with displacement constraints: a bilevel programming approach. *Structural and multidisciplinary optimization*, 14(4):256–263, 1997.

[31] R.V. Kohn and G. Strang. Optimal design and relaxation of variational problems. *Communications on pure and applied mathematics*, 39:113–137(Part I),139–182(Part II),353–377(Part III), 1986.

[32] C. Le, J. Norato, T. Bruns, C. Ha, and D. Tortorelli. Stress-based topology optimization for continua. *Structural and Multidisciplinary Optimization*, 41(4):605–620, 2010.

[33] M. Mrzygłód and A.P. Zieliński. Numerical implementation of multiaxial high-cycle fatigue criterion to structural optimization. *Journal of Theoretical and Applied Mechanics*, 44(3):691–712, 2006.

[34] M. Mrzyglod and AP Zielinski. Multiaxial high-cycle fatigue constraints in structural optimization. *International Journal of Fatigue*, 29(9):1920–1926, 2007.

[35] M. Mrzyglod and AP Zielinski. Parametric structural optimization with respect to the multiaxial high-cycle fatigue criterion. *Structural and Multidisciplinary Optimization*, 33(2):161–171, 2007.

[36] Optistruct. 11.0, users manual. Altair engineering. *Inc., Troy, MI*, 2012.

[37] J. París, F. Navarrina, I. Colominas, and M. Casteleiro. Topology optimization of continuum structures with local and global stress constraints. *Structural and Multidisciplinary Optimization*, 39(4):419–437, 2009.

[38] J. París, F. Navarrina, I. Colominas, and M. Casteleiro. Block aggregation of stress constraints in topology optimization of structures. *Advances in Engineering Software*, 41(3):433–441, 2010.

[39] GIN Rozvany. Difficulties in truss topology optimization with stress, local buckling and system stability constraints. *Structural and Multidisciplinary Optimization*, 11(3):213–217, 1996.

[40] GIN Rozvany. Aims, scope, methods, history and unified terminology of computer-aided topology optimization in structural mechanics. *Structural and Multidisciplinary Optimization*, 21(2):90–108, 2001.

[41] G.I.N. Rozvany. A critical review of established methods of structural topology

optimization. *Structural and Multidisciplinary Optimization*, 37(3):217–237, 2009.

[42] GIN Rozvany and T. Birker. On singular topologies in exact layout optimization. *Structural and Multidisciplinary Optimization*, 8(4):228–235, 1994.

[43] GIN Rozvany, M. Zhou, and T. Birker. Generalized shape optimization without homogenization. *Structural and Multidisciplinary Optimization*, 4(3):250–252, 1992.

[44] O. Sigmund. On the design of compliant mechanisms using topology optimization*. *Journal of Structural Mechanics*, 25(4):493–524, 1997.

[45] O. Sigmund. Topology optimization: a tool for the tailoring of structures and materials. *Philosophical Transactions of the Royal Society of London. Series A: Mathematical, Physical and Engineering Sciences*, 358(1765):211–227, 2000.

[46] O. Sigmund. Morphology-based black and white filters for topology optimization. *Structural and Multidisciplinary Optimization*, 33(4):401–424, 2007.

[47] O. Sigmund. On the usefulness of non-gradient approaches in topology optimization. *Structural and Multidisciplinary Optimization*, 43:589–596, 2011.

[48] O. Sigmund and J. Petersson. Numerical instabilities in topology optimization: a survey on procedures dealing with checkerboards, mesh-dependencies and local minima. *Structural and Multidisciplinary Optimization*, 16(1):68–75, 1998.

[49] MSC Software. MSCFatigue, 2012. http://www.mscsoftware.com.

[50] M. Stolpe and K. Svanberg. An alternative interpolation scheme for minimum compliance topology optimization. *Structural and Multidisciplinary Optimization*, 22(2):116–124, 2001.

[51] G. Strang and R.V. Kohn. Optimal design in elasticity and plasticity. *International journal for numerical methods in engineering*, 22:183–188, 1986.

[52] S. Suresh. *Fatigue of materials*. Cambridge University Press, 1998.

[53] K. Svanberg. The method of moving asymptotes - a new method for structural optimization. *International journal for numerical methods in engineering*, 24(2):359–373, 1987.

[54] K. Svanberg. A class of globally convergent optimization methods based on conservative convex separable approximations. *SIAM Journal on Optimization*, 12(2):555–573, 2002.

[55] K. Svanberg. Some modelling aspects for the fortran implementation of mma. Technical report, Technical Report, 2004.

[56] K. Svanberg and M. Werme. Sequential integer programming methods for stress constrained topology optimization. *Structural and Multidisciplinary Optimization*, 34(4):277–299, 2007.

[57] G. Sved and Z. Ginos. Structural optimization under multiple loading. *International Journal of Mechanical Sciences*, 10(10):803–805, 1968.

[58] Bo Torstenfelt. The trinitas project, 2012. http://www.solid.iei.liu.se/Offered_services/Trinitas.

[59] T. Washizawa, A. Asai, and N. Yoshikawa. A new approach for solving singular systems in topology optimization using krylov subspace methods. *Structural and Multidisciplinary Optimization*, 28(5):330–339, 2004.

[60] M. Werme. Using the sequential linear integer programming method as a post-processor for stress-constrained topology optimization problems. *International journal for numerical methods in engineering*, 76(10):1544–1567, 2008.

[61] RJ Yang and CJ Chen. Stress-based topology optimization. *Structural and Multidisciplinary Optimization*, 12(2):98–105, 1996.

[62] M. Zhou, YK Shyy, and HL Thomas. Checkerboard and minimum member size control in topology optimization. *Structural and Multidisciplinary Optimization*, 21(2):152–158, 2001.